

A Two-Step Refolding of Acid-Denatured Microbial Transglutaminase Escaping from the Aggregation-Prone Intermediate

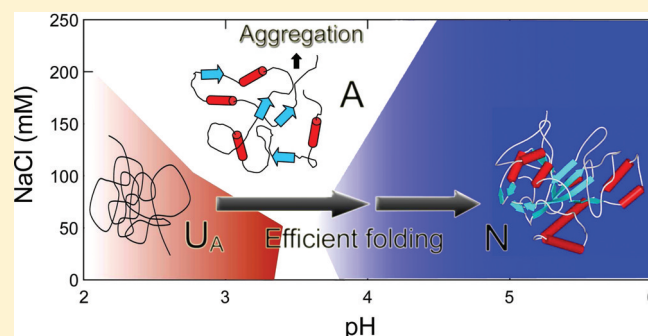
Mototaka Suzuki,^{*,†,‡} Kei-ichi Yokoyama,[†] Young-Ho Lee,[‡] and Yuji Goto^{*,‡}

[†]Institute for Innovation, Ajinomoto Co., Inc., Suzuki-cho 1-1, Kawasaki-ku, Kawasaki 210-8681, Japan

[‡]Institute for Protein Research, Osaka University, Yamadaoka 3-2, Suita, Osaka 565-0871, Japan

Supporting Information

ABSTRACT: Microbial transglutaminase (MTG) is a monomeric globular enzyme made of 331 amino acid residues. The conformation of MTG was examined over the pH 2.0–6.0 region using circular dichroism (CD) and 1-anilino-8-naphthalenesulfonate (ANS). Under conditions of low ionic strength, a decrease of pH below 4 caused a stepwise unfolding with an intermediate exhibiting specific ANS-binding before full unfolding at pH 2.0. At high ionic strength, the decrease of pH led to only an intermediate without further unfolding. The intermediate corresponds to the molten globule state with a secondary structure similar to the native state but disordered tertiary structures. A pH- and NaCl concentration-dependent phase diagram showed that the fully unfolded state exists only under limited conditions of low pH and a low NaCl concentration. Although a refolding yield by the direct jump to pH 6.0 was low, a two-step refolding with incubation at pH 4.0, where MTG is marginally stable, and a subsequent jump to pH 6.0 improved the yield by suppressing the kinetic traps. We propose that the two-step refolding is useful for improving the yield of larger proteins with a high pI value.



Transglutaminases (TGases;¹ protein-glutamine γ -glutamyl-transferases, EC 2.3.2.13) are a family of enzymes that catalyze an acyl transfer between the γ -carboxamide group of glutamine residues within peptides and the ϵ -amino group of lysine residues, resulting in the formation of ϵ -(γ -glutamyl) lysine cross-linkages. TGases are widely distributed in various cells and tissues of mammals, and their physiological properties have been studied.² *Streptomyces mobaraensis* TGase (MTG; microbial transglutaminase), the activities of which were independent of calcium, has been identified, and its enzymatic properties have been characterized.^{3,4} MTG is of interest in regard to not only its structure–function relationship but also its application to food processing.⁵ Purified MTG has been analyzed, and its amino acid residue sequence (331 residues) and pI value (8.0) have been identified.^{6,7} The crystal structure of MTG has also been determined, revealing a single compact domain (Figure S1 of the Supporting Information).⁸

MTG is known to be expressed as a preproenzyme and has been processed to the mature form.⁷ Its pro-region was thought to be essential for efficient protein folding, secretion, and suppression of its enzymatic activity. On the other hand, we reported that MTG without a propeptide sequence expressed as inclusion bodies in *Escherichia coli*⁹ can be efficiently refolded into the active structure although its refolding yield was about 80%.¹⁰ Because MTG is a relatively large single domain globular protein, studying its unfolding and refolding will be useful to obtain further insights into the mechanism of protein

folding and moreover its application to protein engineering. We consider acid denaturation important because it has been systematically investigated,¹¹ revealing a clearer understanding of its molecular mechanism.

In acid denaturation, intramolecular charge repulsion is the dominant driving force for unfolding. Acid-denatured proteins often have two conformational states: the largely unfolded acidic (U_A) state and the relatively compact acidic intermediate (A) with many of the properties of a molten globule.¹¹ The molten globule is a compact denatured form with a significant amount of secondary structure but with a largely disordered tertiary structure.^{12–14} The distribution of the U_A and A states is determined by a balance of charge repulsion which favors fully unfolding and hydrophobic interactions and other specific interactions which favor the A state. Ionic conditions are critical in determining the distribution of the U_A and A states. The binding of the anions, which depends on the ion species, shields the charge repulsion, thus stabilizing the compact A state. It has been suggested that the anion-dependent conformational transition is common to various proteins, particularly those with alkaline pI values.¹¹

Received: July 10, 2011

Revised: October 1, 2011

Published: October 27, 2011



The aims of this paper are twofold. First, we tried to map out the pH- and anion-dependent unfolding transitions of MTG in order to characterize the acid-denatured conformations and the mechanism of unfolding. With a phase diagram of the pH- and NaCl concentration-dependent conformational states, we show that the conformation of the acid-denatured MTG can be explained clearly taking the anion-dependent conformational transition into account. Second, we searched for procedures for the efficient refolding of MTG. Reversible unfolding of a protein with more than 300 amino acid residues is still a challenge although some successful examples have been reported in the REFOLD database (<http://refold.med.monash.edu.au/>) (see Discussion). Then, we propose that a two-step refolding process involving a marginally stable native state at pH 4.0 is a useful approach for refolding the acid-denatured MTG.

EXPERIMENTAL PROCEDURES

Protein Purification. Native MTG was purified from the culture medium of *Streptomyces mobaraensis* as described previously³ and stored in 20 mM sodium phosphate buffer (pH 6.0) at 4 °C. The enzyme was found to be homogeneous by analytical reverse-phase HPLC using a Vydac C4 column (214TP5410, 4.6 mm i.d. × 10 cm, Vidac) as described before.¹⁰

Chemicals. HPLC-grade solvents were purchased from Nacalai Tesque (Kyoto, Japan). TFA (analytical grade) was from Wako Life Science (Osaka, Japan). All other chemicals were of reagent grade.

Circular Dichroism and Fluorescence Measurements. All measurements were carried out at 25 °C with thermostatically controlled cell holders. Circular dichroism (CD) measurements were made with a Jasco spectropolarimeter, Model J-720 or J-820. The instruments were calibrated with D-camphorsulfonic acid. The results are expressed as mean residue ellipticity $[\theta]$, which is defined as $[\theta] = 100\theta_{\text{obs}}/lc$, where θ_{obs} is observed ellipticity in degrees, c is the concentration in residue moles per liter, and l is the length of the light path in centimeters. The CD spectra were measured at protein concentrations of 1.7–3 μM (0.1–0.2 mg/mL) with a 1 mm path length cell from 250 to 190 nm and 1.7–3 μM with a 10 mm path length cell from 320 to 240 nm. Fluorescence spectra were measured with a Hitachi fluorescence spectrophotometer, F3000. 1-Anilino-8-naphthalenesulfonate (ANS) fluorescence was measured with excitation at 400 nm and with less than 0.1 absorbance unit at the excitation wavelength.

Conformational Transitions. The acid-dependent conformational transitions were measured by CD spectroscopy at 25 °C. The native MTG at a protein concentration of about 30 μM (2.0 mg/mL) was dialyzed against 1 mM sodium phosphate (pH 6.0) for 15 h at 4 °C and then diluted 10-fold with buffer solutions at 25 °C. The buffer solutions used were 20 mM sodium phosphate between pH 2.0 and 3.5, and 6.0, and 20 mM sodium acetate between pH 3.5 and 5.0.

The salt-dependent conformational transitions were measured by CD spectroscopy in the absence and presence of sodium chloride (NaCl). The experimental procedure was as described above. The concentrations of NaCl were adjusted to 50–500 mM after dilution. ANS was added to the protein solutions at 25 °C in the absence or presence of NaCl at different pH. The protein concentration was 3 μM . The fluorescence measurements were made 1 h after the solution was prepared.

Buffer Exchange and Refolding of MTG. A PD-10 (GE Healthcare Bio-Sciences, Sweden) column was equilibrated with 10 mM HCl (pH 2.0) at 25 °C. The 10 μM (about 0.7 mg/mL) of native MTG was applied to the column and eluted with 10 mM HCl. MTG was collected from the eluate by detection of absorbance at 280 nm and incubated for 12 h at 4 °C to unfold. Acid-unfolded MTG, the concentration of which was 5–6 μM (0.3–0.4 mg/mL), was diluted 2-fold with 100 mM sodium phosphate buffer at pH 3.0 and 6.0, and 100 mM sodium acetate buffer between pH 3.5 and 5.0, and held at 4 °C for 2 h. To examine the conformational change of the native MTG upon the decrease in pH, a PD-10 column was also used for exchanging the buffer.

To investigate the temperature dependence of refolding, MTG after the jump to pH 4.0 was held at 25 or 37 °C for 2 h. The pH values were measured after refolding. The solutions containing refolded MTG were adjusted to pH 6.0 by the addition of 1 M sodium hydroxide (NaOH) at each temperature and held for 12 h at 4 °C.

N-carbobenzoxy-L-glutamylglycine (CBZ-Gln-Gly), a substrate of TGase,¹⁵ was tested for its potential to enhance the refolding yield. Acid-unfolded MTG at 5–6 μM was diluted 2-fold with 100 mM sodium acetate buffer at pH 4.0 and held at 4 °C for 2 h. CBZ-Gln-Gly was added to a final concentration of 1–1000 μM and incubated for an additional 2 h at 4 °C. The solutions containing refolded MTG were adjusted to pH 6.0 by the addition of 1 N NaOH at 4 °C.

After incubating overnight, the solutions were centrifuged and filtrated with a double layer (hydrophobic top and hydrophilic bottom) nonsterile 0.45 μm filter (Kurabo, Japan). The enzymatic activity of MTG was measured by the colorimetric hydroxamate procedure using CBZ-Gln-Gly. Buffer A consisted of 30 mM CBZ-Gln-Gly, 100 mM hydroxylammonium chloride, 10 mM glutathione (reduced form), and 50 mM Mes (pH 6.0). Buffer B consisted of 1 N HCl, 4% trichloroacetic acid, and 5% iron(III) chloride hexahydrate. A 100 μL sample was incubated in 1.0 mL of buffer A at 37 °C, and the reaction was terminated by the addition of 1.0 mL of buffer B. The absorbance of the samples was measured at 525 nm using a Shimadzu pharmaspec UV-1700 UV-vis spectrophotometer. One unit was defined as the formation of 1 μmol of hydroxamate acid per minute. L-Glutamic acid γ -monohydroxamate was used as a standard. The protein concentration of MTG was determined spectrophotometrically by using a molar absorption coefficient at 280 nm of 74 025.¹⁶ The yields of protein recovery and enzymatic activity were determined by comparing the resulting protein amount and enzymatic activity with the initial values, respectively.

Analytical Ultracentrifugation Measurements. Sedimentation velocity data were obtained using a Beckman-Coulter Optima XL-I analytical ultracentrifuge with an An-60 rotor and two-channel, charcoal-filled Epon cell for six samples. Samples were diluted to about 5 μM (0.3 mg/mL) using their corresponding buffer. All experiments were performed at 4 °C. The absorbance data at 280 nm were collected at 10 min intervals by centrifugation at 181000g (52000 rpm) after incubation for 5 min at 27000g (20000 rpm) at 4 °C. The experimental sedimentation coefficients were obtained by analyzing the sedimentation velocity data and corrected to $s_{20,w}$ (standard solvent conditions: the density and velocity of pure water at 20 °C) using the software UltraScan 8.0.

Dynamic Light Scattering Measurements. All dynamic light scattering (DLS) measurements were performed using a

Zetasizer instrument (DynaPro; Wyatt Technology Corporation) at 4 °C using a standard cuvette of 1 cm path length. Samples were diluted to about 6 μ M (0.26 mg/mL) using their corresponding buffer as described above. The samples with and without filtration using MILLEX GV filter (0.22 μ m) were prepared, and measurements were done twice (after 10 min and 24 h). Scattering data were collected as an average of 30 scans collected over 300 s. The data were processed in accordance with the manufacturer's software (DYNAMICS; Wyatt Technology Corporation) and presented as scattering intensity of an exponentially decaying autocorrelation. The Stokes–Einstein relationship, together with refractive indices and temperature corrected viscosities provided by the DYNAMICS software, was used to calculate the hydrodynamic radius of the aggregates.

RESULTS

Acid Denaturation of MTG. The acid denaturation of MTG was monitored using the CD spectra (Figure 1A). The far- and near-UV CD spectra at pH 4.0 were similar to those at pH 6.0, confirming that the conformation of MTG is stable at pH 4.0–6.0.¹⁷ At pH 2.0 in the absence of salt, the spectrum showed a large negative trough at 200 nm, characteristic of the U_A state. The CD spectrum in the aromatic region at pH 2.0 was essentially featureless, indicating the absence of a native-like tertiary structure.

We examined the conformation of MTG by ANS (Figure 1C). The fluorescence intensity of ANS is known to increase when the dye binds to hydrophobic regions of a protein.¹⁸ On the other hand, ANS binds minimally to the native or unfolded states.¹³ The change in the fluorescence of ANS in the presence of the native state at pH 6.0 and the acid unfolded state at pH 2.0 was negligible (Figure 1C), confirming that MTG is substantially unfolded under the acidic conditions in the absence of salt.

Although the CD spectrum at pH 2.0 in the absence of salt showed substantial unfolding, in the presence of 200 mM NaCl, the far-UV spectrum was similar to that of the native state (Figure 1B). On the other hand, the spectrum in the near-UV region was distinct from that of the native state but similar to that of the U_A state without fine peaks (Figure 1B). These results indicate that, in the presence of 200 mM NaCl, an intermediate state with a native-like secondary structure but with substantially disordered side chains accumulates. The fluorescence spectrum of ANS showed a large increase in intensity upon addition of NaCl at pH 2.0 (Figure 1C). The emission maximum shifted from 540 to 470 nm, indicating the burial of the ANS molecules in a hydrophobic environment.¹⁹ In several cases, the extensive binding of ANS has been used to confirm the accumulation of molten globule states.^{13,14}

To address the effects of salt in detail, we examined the acid-induced transition under different conditions monitored by measuring ellipticity at 222 nm (Figure 2A–D). When the pH was lowered in the absence of NaCl, the acidic transition occurred apparently as a single transition between pH 3.0 and 4.0 (Figure 2A). In the presence of 50 mM NaCl, the transition was similar to that in the absence of salt (Figure 2A,B). In 100 mM NaCl, the transition shifted to lower pH regions (i.e., pH 3.0 to 2.5) with less of a change in ellipticity (Figure 2C). In 200 mM NaCl, the transition monitored at 222 nm disappeared, although a transient decrease in ellipticity was observed at around pH 4.0, due to the aggregation of MTG (see below) (Figure 2D). In the presence of 500 mM NaCl, the

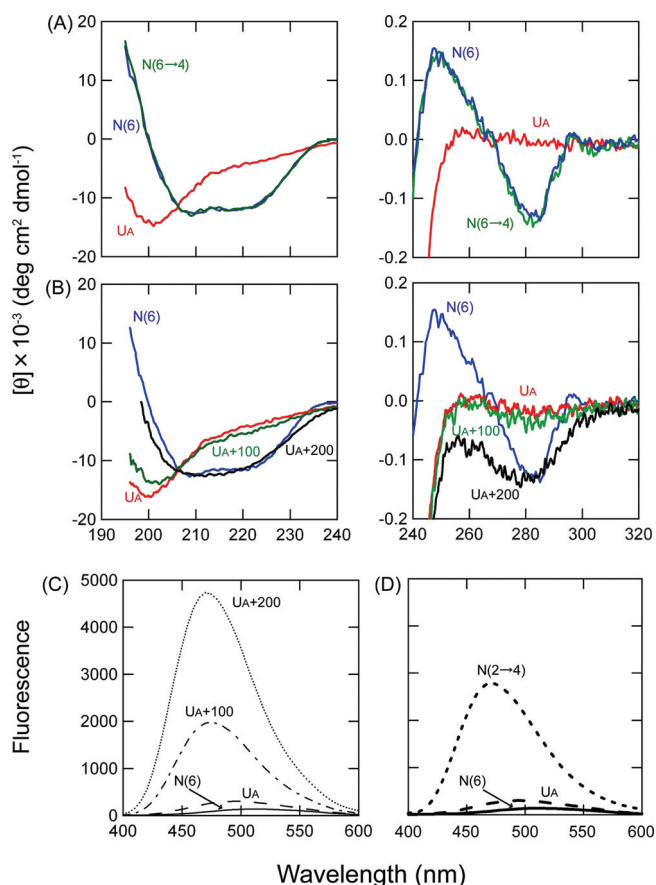


Figure 1. Conformational transitions of MTG monitored by CD and ANS fluorescence spectra at 25 °C. (A) Far- and near-UV CD spectra at pH 6.0 (N(6)), pH 4.0 (N(6→4)), and pH 2.0 (U_A). Protein concentrations were 3 μ M. (B) Dependence on the NaCl concentration of far- and near-UV CD spectra at pH 2.0. NaCl concentrations were 0 (U_A), 100 ($U_A + 100$), and 200 ($U_A + 200$) mM. The spectrum at pH 6.0 in the absence of salt (N(6)) was shown for comparison. The measurements were performed soon after preparation of the solution. (C) Dependence on the NaCl concentration of fluorescence spectrum of ANS at pH 2.0. The concentrations of MTG and ANS were 3 and 20 μ M, respectively. The concentrations of NaCl were 0 (U_A), 100 ($U_A + 100$), and 200 ($U_A + 200$) mM. (D) Fluorescence spectrum of ANS in the presence of refolded MTG at pH 4 (N(2→4)). In (C, D), fluorescence spectra of ANS in the presence of native MTG at pH 6.0 (N(6)) and the acid-unfolded MTG at pH 2.0 (U_A) were also shown. The measurements were performed 1 h after preparation of the solution. Excitation was at 400 nm.

acid-induced transition led to aggregation below pH 4.0, revealing that the salt-stabilized intermediate is prone to aggregate. These results show that although the ellipticity at 222 nm is a useful probe for monitoring the acid denaturation, it does not distinguish between the native and intermediate states.

We then used the ANS fluorescence at 484 nm to monitor the acid denaturation under the same conditions as used for the far-UV CD measurements (Figure 2E–H). Unexpectedly, even in the absence of NaCl, three phases were observed (Figure 2E). First, no ANS binding was observed between pH 6.0 and 4.0, where the native state populates. Second, a marked increase of ANS fluorescence occurred between pH 3.0 and 4.0 with a maximum at pH 3.5, revealing the accumulation of the intermediate. Third, no ANS binding was again observed

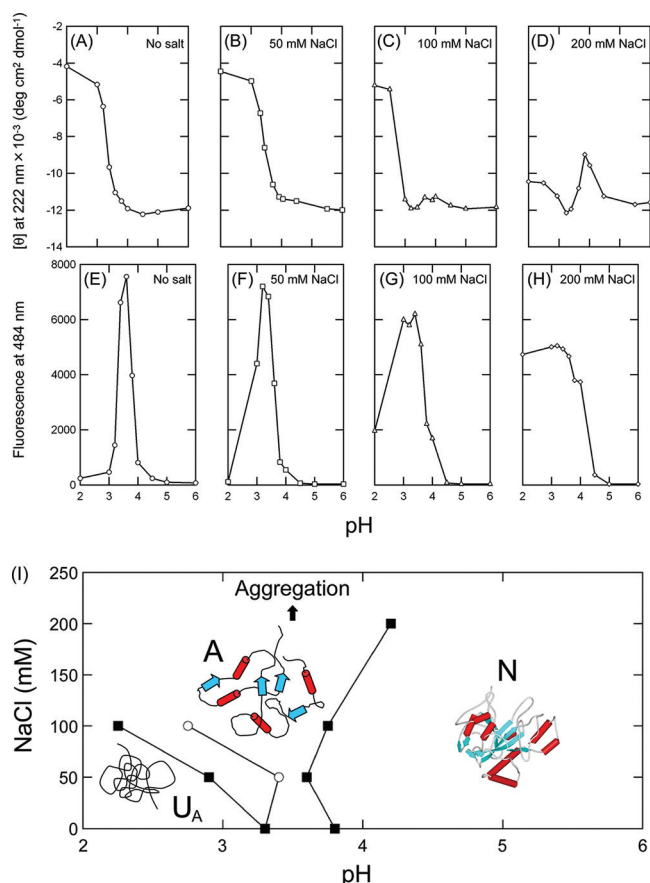


Figure 2. Acid-induced conformational transitions of MTG (A–H) and the phase diagram of the N, A, and U_A states (I) at 25 °C. The transitions under various concentrations of NaCl were measured by the ellipticity at 222 nm (A–D) and the ANS fluorescence at 484 nm (E–H). The concentration of NaCl was indicated in the panels. Conditions for the CD and fluorescence measurements were as described in Figure 1. At the midpoint of the conformational transition, populations of two conformational states are 50%, representing the boundary of the phase transition. Thus, the midpoints of the pH-dependent transitions monitored by CD (○) and ANS fluorescence (■) were plotted. The schematic structure of N state in the phase diagram was produced with the PDB file (1IU4) using ViewerPro 4.2 (Accelrys Inc.).

below pH 3.0, confirming the complete acid unfolding. Although the marked ANS binding at between pH 3.0 and 4.0 was unexpected, the results are consistent with those obtained at 222 nm if we assume that the ellipticity cannot distinguish the native and intermediate states. ANS binds strongly to the intermediate but not at all to the native or fully unfolded state. It is clear that the addition of salt stabilizes the intermediate even at lower pH (Figure 2F–H). In the presence of 200 mM NaCl, the acid denaturation does not produce the fully unfolded state, only leading to the intermediate.

Combining these two types of probes distinguishing the conformational states, we estimated the populations of the native (N), acidic intermediate (A), and acid-unfolded (U_A) states. On the basis of the midpoints of the transitions, we constructed a phase diagram of the three states as a function of pH and NaCl at 25 °C (Figure 2I). The phase diagram shows that the boundary between the N and A states is relatively insensitive to ionic strength. The boundary between the A and U_A states is slightly dependent on the concentration of NaCl,

requiring a higher NaCl concentration for the stabilization of the A state with a decrease of pH. The phase diagram shows that the U_A state accumulates only in a limited area of low ionic strength below pH 3.0. On the other hand, the A state is a dominant form prevailing at a wide range of acidic pH and NaCl concentrations.

Refolding of Acid-Unfolded MTG. Urea-denatured MTG extracted from inclusion bodies has been refolded by a stepwise procedure consisting of the dilution of urea at pH 4.0 and a subsequent jump to pH 6.0 with a refolding yield of about 80% in terms of enzymatic activity.¹⁰ However, dilution of urea increases the volume of the system, requiring several processes. To search for a more convenient and efficient approach for refolding MTG, we examined the refolding starting from the U_A state, exhibiting minimal propensity to aggregate.

Because the direct jump from pH 2.0 to a neutral pH was not effective (see below), the acid-unfolded MTG at pH 2.0 in the absence of salt was refolded by a two-step procedure of increasing pH at 4 °C. In the first step, acid-unfolded MTG (6 μ M; 0.4 mg/mL) was diluted 2-fold by using various pH buffer solutions (pH 2.8–5.5) and incubated for 2 h. In the second step, those solutions were titrated to pH 6.0, where MTG is highly stable, and incubated for 15 h. Refolding was monitored by the enzymatic activity and the protein recovered in the soluble fraction after centrifugation (Figure 3A).

It was found that the direct jump to neutral pH prevents efficient refolding: The first jump to pH 5.5 gave a low enzymatic yield of 13%. The final yields in activity and protein recovery were much higher when the first jump was at slightly acidic conditions, with a maximum increase of about 40% in enzymatic activity and 85% in protein recovery at around pH 4.0. On the basis of these values, fully refolded MTG with full activity is 40%, monomeric misfolded MTG without activity (possibly including small aggregates) is 45% (= 85% – 40%), and the precipitated large aggregates are 15%. The results also indicated that even under the optimal conditions at around pH 4.0, only a half of the recovered (soluble) protein was enzymatically active, suggesting that the low refolding yield is caused by both intra- and intermolecular non-native interactions which prevent refolding to the native state.

To improve the refolding yield, we examined several factors. First, the dependence on temperature during the incubation for 2 h at pH 4.0 showed that the protein recovery decreased drastically from 86% to 19%, when the temperature was raised from 25 to 37 °C (Figure 3C). Because hydrophobic interactions become stronger with an increase in temperature,²⁰ the results argue that too strong hydrophobic interactions cause both intra- and intermolecular non-native interactions. Enzymatic activity was more sensitive than protein recovery, decreasing to 10% at 37 °C.

So far, we incubated for 2 h at pH 4.0 and 4 °C after the first pH jump. Second, the dependence on the incubation period at pH 4.0 was examined (Figure 3E). Both the enzymatic and protein recoveries depended on the incubation period, reaching a plateau at about 60 min. The results were consistent with the observation that the direct jump to neutral pH prevents efficient refolding (Figure 3A). Protein recovery and enzymatic yield changed little upon further incubation (~4 h, Figure 3E).

Third, the effects of CBZ-Gln-Gly, a substrate of MTG,¹⁵ on the refolding at pH 4.0 and 4 °C were examined (Figure 3B). The enhancement of the refolding yields in the presence of 1 mM CBZ-Gln-Gly was moderate: the enzymatic activity

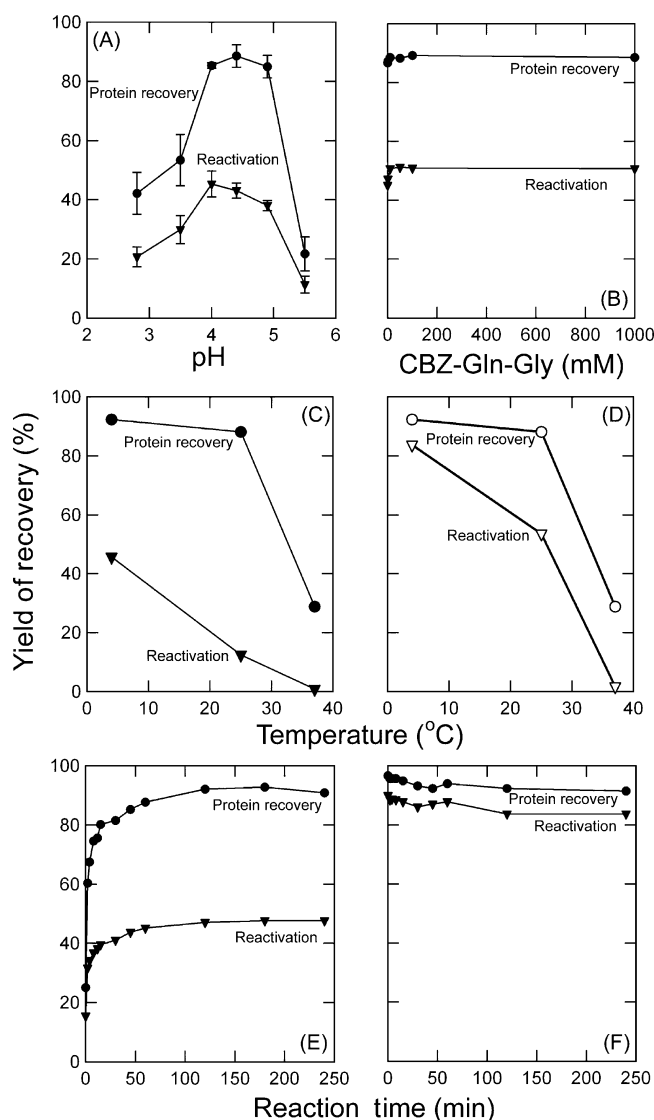


Figure 3. Examination of the factors affecting the refolding yield. (A) Refolding yields of MTG by a two-step refolding at 4 °C. Acid-unfolded MTG was refolded by a two-step refolding through the incubation for 2 h at indicated pH and then for 16 h at pH 6.0. Protein recovery was determined by UV absorbance after precipitation of large aggregates. Activity yield was determined by the relative initial catalytic rate as described in Experimental Procedures. All values were normalized to the initial catalytic rate of native MTG. The experiments were performed on the same day with same batch of proteins. Data were expressed as mean \pm SD ($n = 6$). (B) Dependence on the concentration of CMZ-Gln-Gly present during the 2 h incubation at pH 4.0. After incubation at pH 4.0, pH was jumped to 6.0 with 1 N NaOH and then protein recovery and reactivation yields were measured. (C) Dependence on the temperature of the 2 h incubation at pH 4.0. (E) Dependence on the incubation time at pH 4.0. (D, F) For comparison, the temperature dependence (D) and the time-dependent change of the protein recovery and enzymatic activity (F) after lowering the native MTG at pH 6.0 to pH 4.0 were examined. All experiments were performed at 4 °C.

increased by $\sim 6\%$, but no significant change was observed with respect to the protein recovery. Because the concentration of CBZ-Gln-Gly was low (i.e., 1 mM), it may not have been high enough to have notable effects on the refolding kinetics. However, the addition of a higher concentration of CBZ-Gln-

Gly during refolding tended to cause the aggregation of MTG, making an exact analysis difficult.

Conformation and Activity of the Native MTG at pH 4.0. Although the incubation at pH 4.0 seems to be essential for efficient refolding, it is also likely that the stability of the native MTG at pH 4.0 critically controls the refolding yields. Thus, we examined the conformation and activity of the native MTG at pH 4.0.

When the pH was reduced from 6.0 to 4.0 at 4 °C, the protein recovery after centrifugation and enzymatic activity remained about 90% even after several hours (Figure 3F), indicating that no significant change occurs at pH 4.0 and 4 °C. However, when the incubation temperature was increased, the protein recovery and enzymatic activity decreased remarkably (Figure 3D). These results indicate that MTG at pH 4.0 becomes unstable even at 25 °C, resulting in aggregation and an inactive conformation.

Conformation of Refolded MTG and Intermediates.

The CD spectra of MTG refolded at pH 4.0 and 6.0 by a two-step jump were compared with the spectrum of the native MTG at pH 6.0 (Figure 4A). The far- and near-UV CD spectra

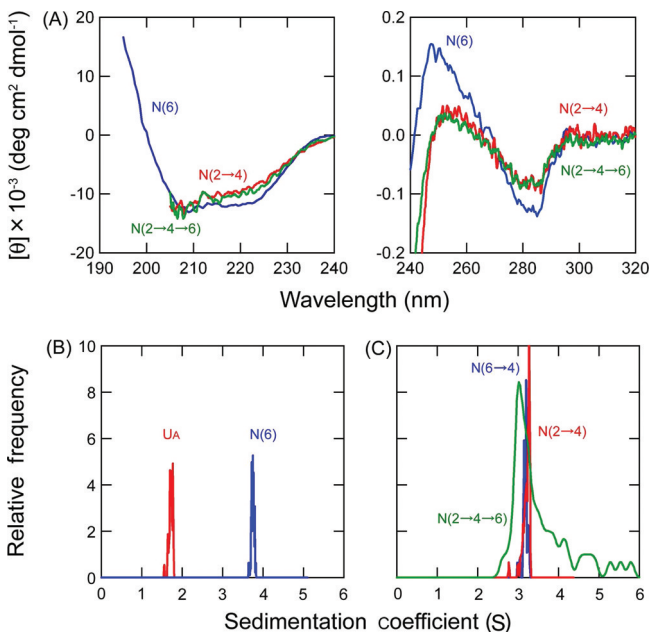


Figure 4. Far- and near-UV CD spectra and sedimentation coefficients of refolded MTG. (A) The spectra of refolded MTG at the first pH jump to pH 4.0 (N(2 \rightarrow 4)) and the second pH jump to pH 6.0 (N(2 \rightarrow 4 \rightarrow 6)) and the native state at pH 6.0 (N(6)) are shown. Protein concentration was 3 μ M. (B, C) The distribution of sedimentation coefficients ($s_{20,w}$) obtained from sedimentation velocity data at 4 °C. (B) The acid-unfolded (U_A) and native MTGs (N(6)). (C) Two types of MTG at pH 4.0, N(2 \rightarrow 4) refolded from acid-unfolded state at pH 2.0, the other N(6 \rightarrow 4) transferred from pH 6.0, and refolded MTG at pH 6, N(2 \rightarrow 4 \rightarrow 6).

of the refolded MTG in the second step at pH 6.0 were similar to those in the first step at pH 4.0, indicating that the major structural change completed after 2 h at pH 4.0. Nevertheless, the CD spectra of the refolded MTG at pH 4.0 or 6.0 were distinct from the spectrum of the native MTG at pH 6.0, especially in the intensity of aromatic peaks at 250 and 280 nm. The results are consistent with the observation that the

refolded MTG contains a significant amount of intra- and intermolecular misfolded species.

The molecular shapes of MTG under different pH conditions were examined by a sedimentation velocity analysis with analytical ultracentrifugation (Figure 4B,C). Sedimentation velocity experiments were conducted for five samples at 6 μ M MTG and 4 °C: (1) native MTG at pH 6.0 (N(6)), (2) acid-unfolded MTG at pH 2.0 (U_A), two types of MTG at pH 4.0, (3) one refolded from the acid-unfolded state (N(2 \rightarrow 4)) and (4) the other prepared from the native state at pH 6.0 by decreasing the pH (N(6 \rightarrow 4)), and (5) MTG at pH 6.0 refolded by a two-step process (N(2 \rightarrow 4 \rightarrow 6)). The centrifugation was conducted at 181000g after a preliminary centrifugation at 27000g. The movements of the boundary of samples during the centrifugation at 181000g were recorded, and the sedimentation coefficient was estimated.

The sedimentation coefficient of N(6) was 3.8, consistent with a globular protein made of 331 amino acid residues (Figure S2 of the Supporting Information). The main component of U_A had a sedimentation coefficient of 1.8, smaller than that of N(6) (Figure 4B). These results indicate that the native MTG is more compact than the acid-unfolded MTG. The sedimentation coefficient of N(2 \rightarrow 4) was 3.2, similar to that of the native MTG at pH 6.0 (Figure 4C). In addition, this value was similar to that of the native MTG at pH 4.0 transferred from pH 6.0 (N(6 \rightarrow 4)). However, because the large aggregates were removed during the prescan for 5 min at 27000g, we also performed the DLS measurements for N(2 \rightarrow 4) (see below). The sedimentation coefficient of the refolded MTG at pH 6.0 (N(2 \rightarrow 4 \rightarrow 6)) showed a significant distribution, indicating that the solution also contains various oligomeric forms and aggregates.

To further address the aggregational propensity of N(2 \rightarrow 4), we performed the DLS measurements at 4 °C with and without filtration by 0.22 μ m membrane filter (Figures S3 and S4 of the Supporting Information). The measurements were done immediately and 24 h after the preparation of the solution. The dead time of immediate measurements was about 10 min. For both time periods, the protein recovery estimated by the difference of the absorbance with and without filtration suggested the formation of large aggregates by 7–8% (Table S1 of the Supporting Information). Interestingly, N(2 \rightarrow 4) immediately after the pH jump dominantly consists of soluble aggregates and the size of aggregates decreases upon incubation at pH 4.0. The results are in agreement with the incubation time dependence of the refolding yield (Figure 3E), indicating that the transient aggregation at pH 4.0 prevents the efficient refolding of MTG. Yokoyama et al.¹⁷ reported that, in the case of refolding from urea-unfolded state, the aggregates which determine the refolding yield accumulates transiently at pH 4.0 monitored by gel filtration chromatography. Thus, the aggregation of the intermediate at pH 4.0 is common to both urea-induced unfolding and acid-induced unfolding and is important for determining the refolding efficiency. However, the current approach using simple pH jump may have several advantages as discussed later (see Discussion).

We confirmed the strong ANS binding to N(2 \rightarrow 4) (Figure 1D) compared with the native or the acid-unfolded MTG. ANS binding to the native MTG at pH 4.0 transferred from pH 6.0 (N(6 \rightarrow 4)) was small (Figure 2B). The results suggest that the refolded MTG at pH 4.0 contains misfolded or aggregated species even though the sedimentation analysis suggested the

monomeric compact conformation, consistent with the DLS results.

On the basis of the results from CD, sedimentation coefficient, DLS, and enzymatic and protein recoveries, we conclude that although the major species of refolded MTG at pH 6.0 under optimal conditions is a monomeric native MTG (40% of the total), it also contains a notable amount of misfolded monomeric MTG (40%) and intermolecularly misfolded aggregates (20%).

DISCUSSION

Conformational Stability under Acidic Conditions.

MTG is a large monomeric globular enzyme made of 331 amino acid residues (Figure S1 of the Supporting Information) whose conformational stability under acidic conditions has been largely unknown. On the basis of acid denaturation monitored using CD and ANS, we constructed a phase diagram consisting of the N, U_A , and A states (Figure 2I). The substantially unfolded U_A state accumulates only under limited conditions: a pH below 3 and NaCl concentration below 100 mM. On the other hand, the A state with properties similar to the compact molten globule state prevails between pH 4.0 and 3.0 in the absence of NaCl and below pH 4.0 in the presence of NaCl above 100 mM. The A state has an overall secondary structure similar to the native state but disordered side chains.¹⁴ It has exposed hydrophobic surfaces as shown by the ANS binding^{13,21} and, consequently, tends to have a high propensity to aggregate.²¹ Indeed, the A state of MTG exhibited high aggregation in the presence of NaCl above 500 mM (data not shown). The phase diagram confirms that the conformational stability of MTG under acidic conditions can be determined by the balance of the charge repulsion favoring unfolding and various forces stabilizing the folded state as established for various small globular proteins.¹¹

Efficient Refolding from Acid Denaturation. Considering the large size of MTG, efficient refolding after denaturation is a challenge. Indeed, the A state of MTG showed a high propensity to aggregate. The reversible unfolding of a globular protein of more than 300 amino acid residues is difficult in general. For example, the unfolding of maize ferredoxin-NADP⁺ reductase with 314 residues, a monomeric globular protein, is irreversible.²² Rhodanese, a mitochondrial protein of 293 amino acid residues, has been often used as a model for protein folding, because the refolding yield of this enzyme is very low but increases significantly when the folding is assisted by molecular chaperones.²³ Refolding protocols for a wide range of proteins have been available at the REFOLD database (<http://refold.med.monash.edu.au/>). The REFOLD database shows the refolding protocols for about 1000 proteins, of which 296 are proteins larger than 330 amino acid residues. Among the 296 proteins, 35 were reported with refolding yields: 14 proteins with more than 40% yield and two (cyclomaltodextrin glucanotransferase²⁴ and lipase²⁵) with 100% yield. However, checking the papers, we found that the exact refolding yields of cyclomaltodextrin glucanotransferase and lipase were 40% and 33%, respectively. At this stage, refolding of a larger protein with more than 300 amino acid residues is really challenging.

β -Lactamase with 290 residues is a case similar to MTG with a high pI value around 8.0 and largely unfolded conformations at low pH in the absence of salt.¹¹ β -Lactamase also forms the aggregation-prone A state under the high salt conditions at low pH. In the case of β -lactamase, it has been suggested that the

efficient refolding to the native state can be achieved under low salt conditions by evading the aggregation-prone A state.¹¹ Thus, we searched for efficient refolding taking into account the phase diagram of MTG (Figure 2I).

Even starting from the U_A state with minimal propensity to aggregate, the direct jump to slightly acidic pH conditions (i.e., pH 5.5) was not effective. Instead, incubation at pH 4.0, where the native MTG is marginally stable, was necessary for improving the refolding yield. A similar two-step refolding with an incubation at pH 4.0 was also successfully employed for the refolding of urea-denatured MTG.^{5,10} Considering that the stability of MTG increases with the pH, it is likely that overly strong folding forces work adversely, decreasing the refolding yield. To confirm this, it will be important to examine folding kinetics with a stopped-flow apparatus and to examine the effects of point or multiple mutations on avoiding the kinetic trap and thus increasing the refolding yield.

Several examples of strong folding forces preventing efficient refolding have been reported.

(i) In the late 1970s to early 1990s, the role of prolyl *cis*–*trans* isomerization was one of the most important issues in the study of protein folding; however, the kinetic analysis was complicated.^{26–28} Initially, wrong prolyl isomers were thought to prevent folding completely. However, it was found later that the roles of wrong prolyl isomers vary significantly. In the context of this paper, an interesting case has been reported with ribonuclease T1 that, under strongly native conditions, native-like intermediates with wrong prolyl isomers accumulate in which the prolyl isomerization is slowed down because of kinetic trapping.²⁹

(ii) Since the classic work of Anfinsen with ribonuclease A, studying the pathway of the formation of disulfide bonds has been considered important for understanding the mechanism of protein folding. However, studies with the isolated immunoglobulin domain²⁸ and bovine trypsin inhibitor³⁰ showed that under strongly native conditions, protein folding proceeds even without the disulfide bond(s), producing kinetically trapped states without disulfide bond(s). Considering the kinetic trapping induced under strongly native conditions, Tsumoto and co-workers have proposed a stepwise refolding, in which the concentration of denaturant is reduced in stepwise fashion.^{31,32} This technology controls the folding pathway by adjusting the concentrations of the denaturant and other additives to induce sequential folding or disulfide formation without kinetic trapping.

(iii) More recently, to obtain insights into the folding of large proteins, Yagi et al. constructed a bovine β -lactoglobulin (β -lg) dimeric mutant, A34C/C121A β -lg.³³ In the mutant, a free thiol group of wild-type β -lg at Cys121 was removed, and two β -lg molecules were linked by a disulfide bridge through Cys34 created at the dimer's interface. Under strongly native conditions at low concentrations of urea, the refolding yield of A34C/C121A β -lg was low. However, under marginally native conditions, the yield improved notably although the refolding was slow. The results indicated that, if the non-native interactions are too strong, the kinetic trap is set, leading to a glass-like misfolded state.

All the examples summarized above argue for the importance of marginal stability in making possible the folding of large proteins.

Strategies for the Efficient Refolding. Because MTG has been used in the food industry for the modification of proteins,⁵ developing a method of efficient refolding is also

important from a practical viewpoint. Hence, various studies to develop an efficient system for producing MTG have been reported. Liu et al.³⁴ reported on-column refolding of MTG from inclusion bodies with a reactivation yield of ~50%, which is equal to the refolding yield of acid-unfolded MTG reported here. However, because of the chromatographic step, the system is thought to be more complicated and expensive than the current procedures. Previous reports described that a refolding process composed of rapid dilution and pH titration efficiently reactivated urea-denatured MTG extracted from inclusion bodies.^{9,10} Using that process, the reactivation of MTG was ~80%, which is more efficient than the current method employing the acid-unfolding and refolding. However, the cost of the refolding from urea denaturation is higher than the current process because of the large amount of urea and recycling needed. The urea-denatured refolding needed 2 h to reach a plateau in terms of reactivation.¹⁰ The refolding of the acid-unfolded MTG finishes within ~1 h (Figure 3E). Although the pH for urea-denatured refolding was critical,¹⁰ the pH range of acid-unfolded refolding is relatively wide. As a possible tool for improving the refolding yield, various additives can be considered.^{35–37} In the case of bovine liver rhodanase, the reactivation from acid denaturation was dramatically increased by adding an aliquot of detergent, reductant, and substrate.³⁵ Although the effects of CBZ-Gln-Gly on the refolding of MTG were marginal (Figure 3B), it is possible to search for conditions that enhance the effects of additives. Kudou et al.³⁸ reported the refolding yield of MTG was dramatically improved by two kinds of additive: 2.0% C12-L-Glu and 0.8 M arginine. Therefore, if the reactivation procedure could be improved, a rational refolding strategy on the basis of the phase diagram could become a promising approach.

CONCLUSION

MTG is a large monomeric globular enzyme for which reversible unfolding is a challenge. On the basis of the acid denaturation of MTG monitored using CD and ANS, we constructed a phase diagram consisting of the N, U_A, and A states. Largely unfolded U_A state accumulates only under limited conditions: a pH below 3 and NaCl concentration below 100 mM. On the other hand, the A state exhibiting high aggregation propensity prevails under acidic conditions. We then searched for a simple and efficient way of refolding the acid-denatured MTG. We found a two-step procedure through the marginally stable native state at pH 4.0 under low salt conditions to be effective, although the refolding yield was still 40%. Further studies improving the refolding yield of MTG will be useful for understanding the mechanism of protein folding and for applications to protein engineering. Finally, it is likely that the current procedure will be applicable in general to various proteins with a high pI value as previously suggested for β -lactamase.¹¹

ASSOCIATED CONTENT

Supporting Information

Table S1 and Figures S1–S4. This material is available free of charge via the Internet at <http://pubs.acs.org>.

AUTHOR INFORMATION

Corresponding Author

*Tel 81-44-21-5892; Fax 81-44-210-5897; e-mail mototaka_suzuki@ajinomoto.com (M.S.). Tel 81-6-6879-8614; Fax 81-6-6879-8616; e-mail ygoto@protein.osaka-u.ac.jp (Y.G.).

Funding

This work was supported by the Japan Society for the Promotion of Science Research Fellowships for Young Scientists to Y.-H.L.

ACKNOWLEDGMENTS

We thank Miyo Sakai (Institute for Protein Research) for performing ultracentrifuge analysis.

ABBREVIATIONS

ANS, 1-anilino-8-naphthalenesulfonate; β -lg, β -lactoglobulin; CBZ-Gln-Gly, *N*-carbobenzoxy-L-glutaminyglycine; CD, circular dichroism; DLS, dynamic light scattering; MTG, microbial transglutaminase; TGases, protein-glutamine γ -glutamyl-transferase.

REFERENCES

- (1) Ikura, K., Nasu, T., Yokota, H., Tsuchiya, Y., Sasaki, R., and Chiba, H. (1988) Amino acid sequence of guinea pig liver transglutaminase from its cDNA sequence. *Biochemistry* 27, 2898–2905.
- (2) Folk, J. E. (1980) Transglutaminases. *Annu. Rev. Biochem.* 49, 517–531.
- (3) Ando, H., Adachi, M., Umeda, K., Matsuura, A., Nonaka, M., Uchio, R., Tanaka, H., and Motoki, M. (1989) Purification and characterization of a novel transglutaminase derived from microorganisms. *Agric. Biol. Chem.* 53, 2613.
- (4) Nonaka, M., Tanaka, H., Okayama, A., Motoki, M., Ando, H., Umeda, K., and Matsuura, A. (1989) Polymerization of several proteins by calcium-independent transglutaminase derived from microorganisms. *Agric. Biol. Chem.* 53, 2619–2623.
- (5) Yokoyama, K., Nio, N., and Kikuchi, Y. (2004) Properties and applications of microbial transglutaminase. *Appl. Microbiol. Biotechnol.* 64, 447–454.
- (6) Kanaji, T., Ozaki, H., Takao, T., Kawajiri, H., Ide, H., Motoki, M., and Shimonishi, Y. (1993) Primary structure of microbial transglutaminase from *Streptovorticillum* sp. strain s-8112. *J. Biol. Chem.* 268, 11565–11572.
- (7) Pasternack, R., Dorsch, S., Otterbach, J. T., Robenek, I. R., Wolf, S., and Fuchsbaue, H. L. (1998) Bacterial pro-transglutaminase from *Streptovorticillum mobaraense*—purification, characterisation and sequence of the zymogen. *Eur. J. Biochem.* 257, 570–576.
- (8) Kashiwagi, T., Yokoyama, K., Ishikawa, K., Ono, K., Ejima, D., Matsui, H., and Suzuki, E. (2002) Crystal structure of microbial transglutaminase from *Streptovorticillum mobaraense*. *J. Biol. Chem.* 277, 44252–44260.
- (9) Yokoyama, K. I., Nakamura, N., Seguro, K., and Kubota, K. (2000) Overproduction of microbial transglutaminase in *Escherichia coli*, in vitro refolding, and characterization of the refolded form. *Biosci. Biotechnol. Biochem.* 64, 1263–1270.
- (10) Yokoyama, K., Kunio, O., Ohtsuka, T., Nakamura, N., Seguro, K., and Ejima, D. (2002) In vitro refolding process of urea-denatured microbial transglutaminase without pro-peptide sequence. *Protein Expression Purif.* 26, 329–335.
- (11) Fink, A. L., Calciano, L. J., Goto, Y., Kurotsu, T., and Palleros, D. R. (1994) Classification of acid denaturation of proteins: intermediates and unfolded states. *Biochemistry* 33, 12504–12511.
- (12) Ohgushi, M., and Wada, A. (1983) 'Molten-globule state': a compact form of globular proteins with mobile side-chains. *FEBS Lett.* 164, 21–24.
- (13) Semisotnov, G. V., Rodionova, N. A., Kutysenko, V. P., Ebert, B., Blanck, J., and Ptitsyn, O. B. (1987) Sequential mechanism of refolding of carbonic anhydrase B. *FEBS Lett.* 224, 9–13.
- (14) Arai, M., and Kuwajima, K. (2000) Role of the molten globule state in protein folding. *Adv. Protein Chem.* 53, 209–282.
- (15) Folk, J. E., and Cole, P. W. (1966) Mechanism of action of guinea pig liver transglutaminase. I. Purification and properties of the enzyme: identification of a functional cysteine essential for activity. *J. Biol. Chem.* 241, 5518–5525.
- (16) Pace, C. N., Vajdos, F., Fee, L., Grimsley, G., and Gray, T. (1995) How to measure and predict the molar absorption coefficient of a protein. *Protein Sci.* 4, 2411–2423.
- (17) Yokoyama, K., Ejima, D., Kita, Y., Philo, J. S., and Arakawa, T. (2003) Structure of folding intermediates at pH 4.0 and native state of microbial transglutaminase. *Biosci. Biotechnol. Biochem.* 67, 291–294.
- (18) Stryer, L. (1965) The interaction of a naphthalene dye with apomyoglobin and apohemoglobin. A fluorescent probe of non-polar binding sites. *J. Mol. Biol.* 13, 482–495.
- (19) Turner, D. C., and Brand, L. (1968) Quantitative estimation of protein binding site polarity. Fluorescence of N-arylamino-naphthalenesulfonates. *Biochemistry* 7, 3381–3390.
- (20) Makhatadze, G. I., and Privalov, P. L. (1995) Energetics of protein structure. *Adv. Protein Chem.* 47, 307–425.
- (21) Goto, Y., and Fink, A. L. (1989) Conformational states of β -lactamase: molten-globule states at acidic and alkaline pH with high salt. *Biochemistry* 28, 945–952.
- (22) Lee, Y. H., Tamura, K., Maeda, M., Hoshino, M., Sakurai, K., Takahashi, S., Ikegami, T., Hase, T., and Goto, Y. (2007) Cores and pH-dependent dynamics of ferredoxin-NADP⁺ reductase revealed by hydrogen/deuterium exchange. *J. Biol. Chem.* 282, 5959–5967.
- (23) Miyazaki, T., Yoshimi, T., Furutsu, Y., Hongo, K., Mizobata, T., Kanemori, M., and Kawata, Y. (2002) GroEL-substrate-GroES ternary complexes are an important transient intermediate of the chaperonin cycle. *J. Biol. Chem.* 277, 50621–50628.
- (24) Kwon, D. H., Lee, D. H., Han, N. S., and Seo, J. H. (2004) Solid-phase refolding of cyclodextrin glycosyltransferase adsorbed on cation-exchange resin. *Biotechnol. Prog.* 20, 277–283.
- (25) Kojima, Y., Kobayashi, M., and Shimizu, S. (2003) A novel lipase from *Pseudomonas fluorescens* HU380: gene cloning, overproduction, renaturation-activation, two-step purification, and characterization. *J. Biosci. Bioeng.* 96, 242–249.
- (26) Brandts, J. F., Halvorson, H. R., and Brennan, M. (1975) Consideration of the Possibility that the slow step in protein denaturation reactions is due to cis-trans isomerism of proline residues. *Biochemistry* 14, 4953–4963.
- (27) Schmid, F. X. (2005) Prolyl isomerization in protein folding, in *Protein Folding Handbook* (Buchner, J., and Kiefhaber, T., Eds.) pp 916–945, Wiley-VCH, Weinheim.
- (28) Goto, Y., and Hamaguchi, K. (1982) Unfolding and refolding of the constant fragment of the immunoglobulin light chain. *J. Mol. Biol.* 156, 891–910.
- (29) Kiefhaber, T., Grunert, H. P., Hahn, U., and Schmid, F. X. (1992) Folding of RNase T1 is decelerated by a specific tertiary contact in a folding intermediate. *Proteins* 12, 171–179.
- (30) Weissman, J. S., and Kim, P. S. (1991) Reexamination of the folding of BPTI: predominance of native intermediates. *Science* 253, 1386–1393.
- (31) Umetsu, M., Tsumoto, K., Hara, M., Ashish, K., Goda, S., Adschiri, T., and Kumagai, I. (2003) How additives influence the refolding of immunoglobulin-folded proteins in a stepwise dialysis system. Spectroscopic evidence for highly efficient refolding of a single-chain Fv fragment. *J. Biol. Chem.* 278, 8979–8987.
- (32) Tsumoto, K., Arakawa, T., and Chen, L. (2010) Step-wise refolding of recombinant proteins. *Curr. Pharm. Biotechnol.* 11, 285–288.
- (33) Yagi, M., Kameda, A., Sakurai, K., Nishimura, C., and Goto, Y. (2008) Disulfide-linked bovine β -lactoglobulin dimers fold slowly, navigating a glassy folding landscape. *Biochemistry* 47, 5996–6006.

- (34) Liu, X. Q., Yang, X. Q., Xie, F. H., Song, L. Y., Zhang, G. Q., and Qian, S. J. (2007) On-column refolding and purification of transglutaminase from *Streptomyces fradiae* expressed as inclusion bodies in *Escherichia coli*. *Protein Expression Purif.* 51, 179–186.
- (35) Horowitz, P. M., and Xu, R. (1992) Acid pH-induced conformational changes in bovine liver rhodanese. *J. Biol. Chem.* 267, 19464–19469.
- (36) Nomura, Y., Ikeda, M., Yamaguchi, N., Aoyama, Y., and Akiyoshi, K. (2003) Protein refolding assisted by self-assembled nanogels as novel artificial molecular chaperone. *FEBS Lett.* 553, 271–276.
- (37) Rozema, D., and Gellman, S. H. (1995) Artificial chaperons: Protein refolding via sequential use of detergent and cyclodextrin. *J. Am. Chem. Soc.* 117, 2373–2374.
- (38) Kudou, M., Yumioka, R., Ejima, D., Arakawa, T., and Tsumoto, K. (2011) A novel protein refolding system using lauroyl-L-glutamate as a solubilizing detergent and arginine as a folding assisting agent. *Protein Expression Purif.* 75, 46–54.